

Charge-distribution changes accompanying the formation and changes in the composition of HfC_x and TaC_x

G. R. Gruzalski and D. M. Zehner

Solid State Division, Oak Ridge National Laboratory, Oak Ridge, Tennessee 37831-6030

(Received 29 January 1990)

Core-level binding energies (BE's) and valence-band structures, determined with x-ray photoelectron spectroscopy, and C KVV Auger spectra were obtained for TaC_x ($0.5 \lesssim x \lesssim 1.0$) and HfC_x ($0.6 \lesssim x \lesssim 1.0$). In TaC_x the metal $4f$ BE, C $1s$ BE, and the BE of the main p - d valence-band peak decreased (moved toward the Fermi level) as x decreased; in HfC_x these BE's increased as x decreased. In TaC_x the largest BE shift with changing x was for the metal $4f$ BE; in HfC_x it was for the C $1s$ BE. For TaC_x the relative intensity in the valence-band spectra between 0 and 2 eV BE changed significantly as x decreased, eventually becoming the dominant intensity of the spectrum; for HfC_x , deviations from $x \approx 1$ did not change the shape of the valence-band spectra appreciably. The data from both sets of materials are explained in terms of changes in the charge distributions accompanying changes in x . And although the two sets of spectroscopic behavior are quite different, the changes in the charge distributions we are proposing are nevertheless quite similar. In particular, it is proposed that, as x decreases for either HfC_x or TaC_x , the electron charge increases in the vicinity of metal ions and decreases in the vicinity of carbon ions. An analysis of the C KVV Auger spectra is consistent with this interpretation in that the analysis suggests a reduction in C $2p$ -electron occupancy per carbon atom with decreasing x . The $4f$ BE's of Ta and Hf in the elemental metals also were measured and are used to discuss changes in the charge distributions that occur upon formation of HfC_x and TaC_x .

I. INTRODUCTION

Hafnium carbide and tantalum carbide are structurally stable over a very wide range of composition. Their equilibrium phase diagrams indicate that at room temperature they can accommodate carbon deficiencies from near 0% up to about 40% and 20%, respectively, while still maintaining a structure that is basically $B1$ (NaCl). Phases of lower carbon concentrations are not stable for hafnium carbide, but a Ta_2C phase is stable for tantalum carbide. Phases of higher carbon concentrations (other than carbon itself) do not exist in either material, and the solubility for carbon is low in both Hf and Ta. As one might expect, the physical properties of these and other group-IVB and -VB transition-metal carbides strongly depend upon their carbon-to-metal ratio x . Understanding how their electronic structures change with x , and, in particular, how their charge distributions change with x (one focus of this paper), can provide valuable insight concerning concomitant changes in bonding, which affect all physical properties.^{1,2}

In Ref. 3 we reported x-ray-photoelectron-spectroscopy (XPS) data showing that, as x decreased in TaC_x , the C $1s$ binding energy (BE), the Ta $4f$ BE, and the BE of the main (angle-integrated) p - d valence-band peak decreased (shifted toward the Fermi level E_F), and the relative intensity in the valence-band spectra between 0 and 2 eV BE increased. Also presented were C KVV Auger data, which indicated that the number of C $2p$ electrons participating in the Auger process per carbon atom decreased as x decreased. The XPS and Auger-electron-

spectroscopy (AES) data were interpreted in terms of changes in the charge distribution accompanying changes in x . It was concluded that, as x decreased, negative charge accumulated in the vicinity of tantalum ions, in part made up of charge transferred away from carbon ions.

Extending this work, core-level BE's and valence-band structures have been determined from XPS spectra for Hf and for HfC_x over a large range of composition, estimated as $0.6 \lesssim x \lesssim 1.0$, and information concerning differences in the local environments of carbon atoms was determined from C KVV Auger spectra. As was the case for TaC_x , the Auger data from HfC_x indicate a reduction in the number of C $2p$ electrons participating in the Auger process per carbon atom, as x is decreased. Surprisingly, however, it was found that all measured core-level BE's shifted away from the Fermi level as x decreased. Moreover, deviations from stoichiometry ($x = 1$) did not appreciably affect the shape of the XPS valence-band spectra.

In this paper the HfC_x data are presented and compared with those from TaC_x . The data from both sets of materials are explained in terms of changes in the charge distributions accompanying changes in x . Although the two sets of spectroscopic behavior are quite different, the changes in the charge distributions we are proposing are nevertheless quite similar. In particular, it is proposed that, as x decreases for either HfC_x or TaC_x , the electron charge increases in the vicinity of the metal ions and decreases in the vicinity of the carbon ions. The $4f$ BE's of Ta and Hf in the elemental metals also were measured

and are used to discuss changes in the charge distributions that occur upon the formation of HfC_x and TaC_x .

This paper is organized as follows. In Sec. II relevant experimental information is given. The XPS and Auger results are presented in Sec. III and discussed in Sec. IV. Concluding remarks are made in Sec. V.

II. EXPERIMENTAL INFORMATION

Measurements were made in an ion-pumped ultra-high-vacuum (UHV) chamber having a base pressure of less than 10^{-8} Pa and equipped with a double-pass cylindrical mirror analyzer (CMA) containing a coaxial electron gun, an aluminum x-ray source, low-energy electron diffraction (LEED) optics, and a quadrupole mass spectrometer.

The XPS data were obtained with the CMA operated in the retarding mode. The energy scale of the spectrometer was calibrated by setting the measured $\text{Au } 4f_{7/2}$ and $4d_{5/2}$ BE's equal to 84.1 and 335.1 eV, respectively, with the Fermi level being the reference zero.⁴ The Ta and TaC_x spectra were taken using 15-eV pass energy (about 1.2-eV energy resolution), while the hafnium and HfC_x spectra were taken using 25-eV pass energy (about 1.3-eV energy resolution). In both cases, binding energies were determined with an overall estimated precision of ± 0.05 eV. The AES data were obtained with the CMA operated in the nonretarding, first-derivative mode, with 1-V peak-to-peak modulation, which yielded about 0.6% energy resolution.

Crystals of tantalum, tantalum carbide, and hafnium carbide were aligned, cut, and polished to expose (100) surfaces to within 0.3° ; a hafnium crystal was similarly prepared to expose a (0001) surface. In the UHV chamber the crystals were supported by a loop of tantalum wire (0.010 in. diameter); two slots were spark-cut into opposite edges of each crystalline disk to accommodate the wire. An infrared pyrometer was used to monitor approximate surface temperature of the crystals, which were heated by bombarding their back surface with 800-eV electrons.

Near-surface regions of TaC_x and HfC_x of different compositions (and degrees of order) were prepared by first sputtering with argon ions, which left the near-surface region carbon deficient, and then annealing in a controlled manner, which not only allowed the damaged near-surface region to reorder but also allowed carbon to diffuse from the bulk to the surface region, producing a selected near-surface composition. Figure 1 indicates how the average near-surface composition of a sputtered (100) surface of tantalum carbide changed with 10-min anneals. I_C/I_{Ta} is the ratio of the peak-to-peak C KVV Auger signal near 268 eV to the tantalum signal near 163 eV. (Most of the intensity of this Ta signal arises from transitions involving $4d$ holes and $4f$ electrons.) As seen, I_C/I_{Ta} increased with annealing temperatures to about 1200°C , for 10-min anneals. Similar results were obtained for hafnium carbide. A given I_C/I_{Ta} ratio also could be obtained with longer anneals at lower temperatures or with shorter anneals at higher temperatures, consistent with carbon diffusing from the bulk to the near-

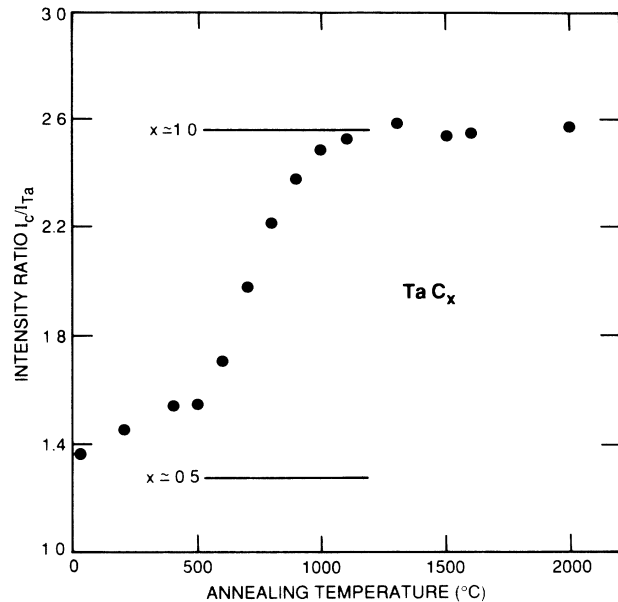


FIG. 1. Auger intensity ratio I_C/I_{Ta} vs annealing temperature for tantalum carbide near-surface regions prepared by argon-ion bombardment (1000 V, $10 \mu\text{A}$, 10 min). Anneals were for 10 min. The two horizontal lines indicating $x \approx 1.0$ and $x \approx 0.5$ were obtained using XPS data as explained in Sec. II.

surface region during an anneal. Most of the surfaces studied in our investigation were prepared with short (≈ 10 s) anneals.

Atomic-sensitivity factors taken from Ref. 5 and areas under XPS C 1s and metal $4f$ peaks were used to determine x , the average carbon-to-metal ratio in the near-surface region. The carbon composition of the sputtered surfaces was $x \approx 0.5$ for TaC_x and $x \approx 0.6$ for HfC_x . For ~ 10 -s anneals, the carbon composition increased with increasing annealing temperature up to $x \approx 1$ for temperatures of about 1800°C for TaC_x and 1600°C for HfC_x . As the annealing temperatures were increased above these values, the near-surface carbon composition did not increase above $x \approx 1$. A value of $x \approx 1$ also was inferred from impact-collision ion-scattering spectra from similarly prepared (100) surfaces of TaC .⁶ Hence, although this XPS method of determining composition often is not accurate, it appears to be so in the case of TaC_x . The two horizontal lines in Fig. 1 were positioned by using this XPS method. In this paper, near-surface regions having $x \approx 1$ are referred to as stoichiometric, even though the term nearly stoichiometric may be more accurate. The bulk compositions of the crystals were previously estimated as being within 1% of stoichiometry.⁷

III. RESULTS

A. Core-level spectra

Shown in Figs. 2(a) and 3(a) are Ta and Hf $4f$ XPS spectra from TaC_x and HfC_x for different carbon-to-metal ratios x . Also shown for comparison are spectra

from clean, well-ordered Ta(100) and Hf(0001). As x decreases, the peaks in the $4f$ spectra from the carbides broaden and the valley regions between the $4f_{5/2}$ and $4f_{7/2}$ peaks fill in, which suggests that the number of distinguishable metal sites is increasing with decreasing x . It is likely that these different sites correspond to metal atoms surrounded by different numbers of carbon atoms.

The Ta $4f$ BE's are significantly larger for elemental tantalum, and they decrease as x decreases. In particular, the $4f_{7/2}$ BE's in TaC_x vary from 23.6 ± 0.05 eV for $x \approx 1$ to 22.8 ± 0.05 eV for $x \approx 0.5$; in elemental Ta the value is 21.6 ± 0.05 eV (see Table I). On the other hand, the Hf $4f_{7/2}$ BE's in HfC_x vary little from the value in elemental Hf, 14.3 ± 0.05 eV,

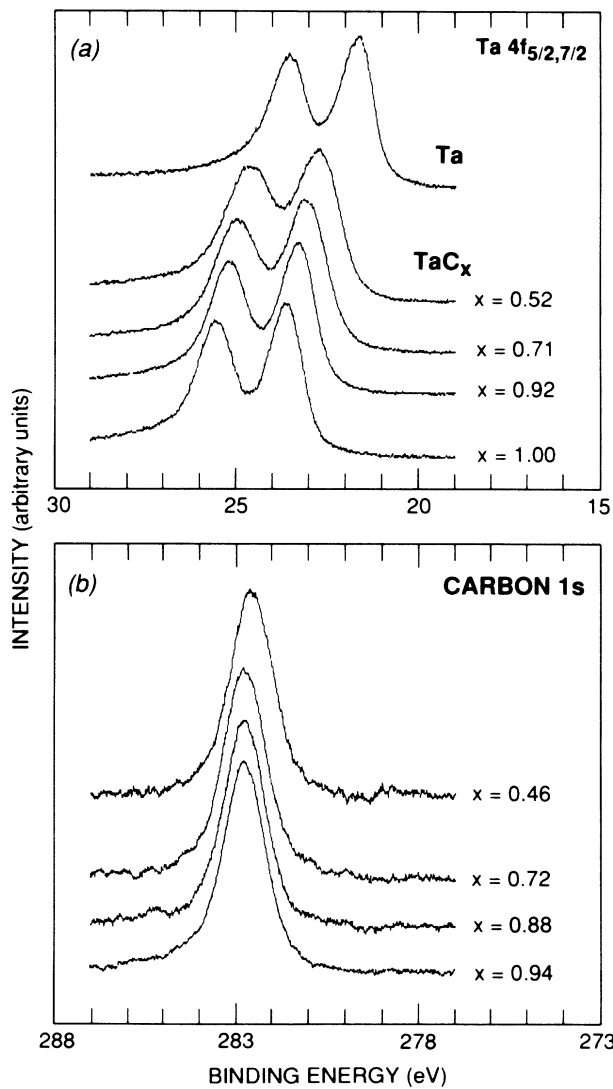


FIG. 2. (a) XPS Ta $4f$ spectra and (b) C $1s$ spectra from tantalum carbide having different carbon-to-metal ratios x . Also shown in (a) is one spectrum from Ta(100). The spectra are normalized so that maximum peak intensities are equal in each figure. Binding energies are with respect to the Fermi level.

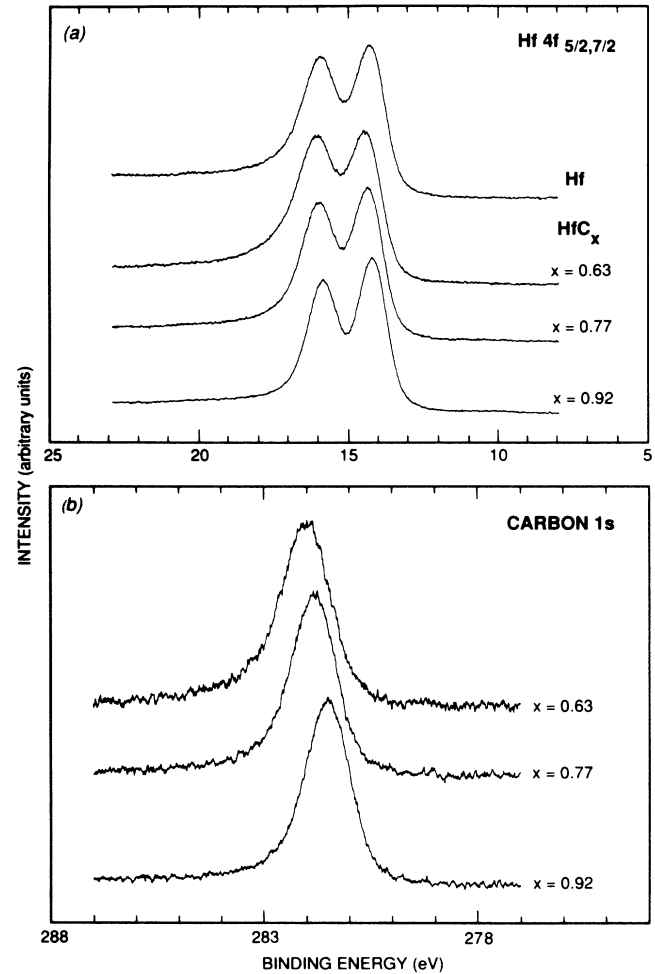


FIG. 3. (a) XPS Hf $4f$ spectra and (b) C $1s$ spectra from hafnium carbide having different carbon-to-metal ratios x . Also shown in (a) is one spectrum from Hf(0001). The spectra are normalized so that maximum peak intensities are equal in each figure. Binding energies are with respect to the Fermi level.

TABLE I. Metal $4f$ and C $1s$ BE's in eV for well-annealed ($x \approx 1$) and as-sputtered ($x < 1$) HfC_x and TaC_x . Also given are the $4f$ BE's in the elemental metals ($x \equiv 0$). BE's were determined with an overall estimated precision of ± 0.05 eV; calibration was performed by setting the measured Au $4f_{7/2}$ and $4d_{5/2}$ BE's equal to 84.1 and 335.1 eV, respectively.

Level	$x \approx 1$	$x \approx 0.6$	$x \approx 0.5$	$x \equiv 0$
HfC_x				
Hf $4f_{7/2}$	14.25	14.45		14.3
C $1s$	281.55	281.95		
TaC_x				
Ta $4f_{7/2}$	23.6		22.8	21.6
C $1s$	282.9		282.6	

and they increase as x decreases, though by only a small amount, from 14.25 ± 0.05 eV for $x \approx 1$ to 14.45 ± 0.05 eV for $x \approx 0.6$. (Binding energies such as 14.25, 14.45 eV, and so on, found here and elsewhere in this paper, do not imply a precision to 0.01 eV; 14.25 eV merely signifies a BE that, to the best of our knowledge, lies approximately midway between 14.2 and 14.3 eV.)

Shown in Figs. 2(b) and 3(b) are C 1s spectra from TaC_x and HfC_x for different values of x . In contrast to the 4f spectra, the 1s spectra do not exhibit significant broadening with decreasing x , consistent with most carbon atoms being surrounded by six metal atoms for all x .

For TaC_x , the C 1s BE decreases from 282.9 ± 0.05 eV for $x \approx 1$ to 282.6 ± 0.05 eV for $x \approx 0.5$; for HfC_x , it increases from 281.55 ± 0.05 eV for $x \approx 1$ to 281.95 ± 0.05 eV for $x \approx 0.6$ eV. Note that, for a given set of materials, the 1s and 4f BE's shift in the same direction as x is varied.

In both sets of materials the separation between C 1s and metal 4f BE's increases with decreasing carbon content. For equal changes in x , however, the increase in separation is larger for TaC_x than for HfC_x . For example, as the carbon content decreases from $x \approx 1$ to $x \approx 0.6$, this separation increases by ~ 0.4 eV for TaC_x and by ~ 0.2 eV for HfC_x .

B. Valence-band spectra

Representative valence-band XPS spectra from TaC_x and HfC_x are compared in Fig. 4. The two lower-lying peaks in the HfC_x spectra (near 4 and 6 eV BE) are due primarily to α_3 and α_4 x-ray satellite excitations of Hf 4f electrons and, therefore, have little to do with the valence band;⁸ corresponding satellite excitations are not visible in the TaC_x spectra because the Ta 4f BE's are larger [cf. Figs. 2(a) and 3(a)]. The valence-band peaks of interest are near 5 eV BE for TaC_x and 3 eV BE for HfC_x ; these are due primarily to photoemission from C 2p and metal 5d states. As x decreases, this peak shifts toward E_F for TaC_x , but away from E_F for HfC_x .

The most striking change in the valence-band spectra for TaC_x is the increase in the relative intensity between 0 and 2 eV BE with decreasing x . For $x \approx 0.97$ the peak just below E_F is small with respect to the one near 5 eV BE; for $x \approx 0.52$ the peak just below E_F is the dominant one in the spectrum. As x decreases for HfC_x , on the other hand, little additional intensity is detected just below E_F . It should be noted that valence-band spectra of TaC_x calculated by Schadler *et al.*⁹ are in fair agreement with those shown in Fig. 4.

A schematic representation of the core-level and valence-band spectra is given in Fig. 5.

C. Carbon KVV Auger spectra

For both HfC_x and TaC_x , the intensity in the higher-energy portions of the C KVV Auger spectra (corresponding to energies above ~ 265 eV for HfC_x and ~ 262 eV for TaC_x) decreases relative to that in the lower-energy portions (corresponding to energies below ~ 255 and ~ 252 eV, respectively) as the carbon content de-

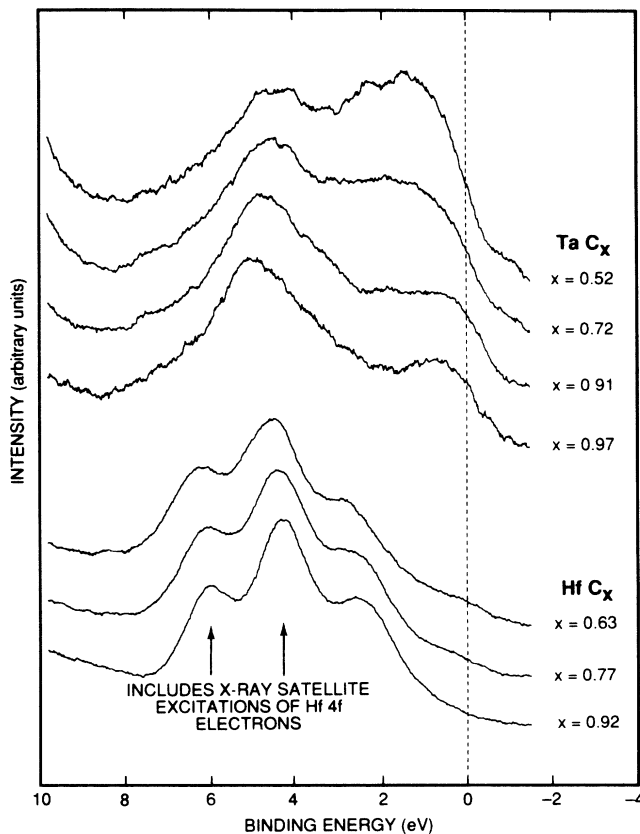


FIG. 4. XPS valence-band spectra from TaC_x and HfC_x having different carbon-to-metal ratios x . The spectra are shown only to 9.8 eV BE, so contributions from C 2s states are not shown. The spectra are normalized so that maximum intensities within each group of spectra are equal.

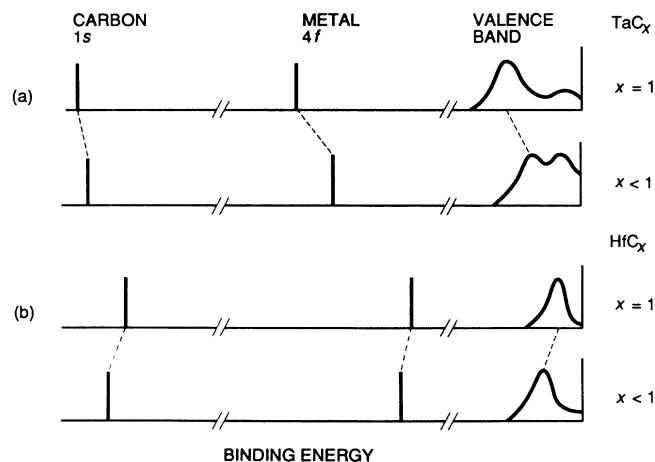


FIG. 5. Schematic of XPS results presented in this paper. Binding energies are with respect to the Fermi level, which is denoted by the vertical (ordinate) axis at the far right of each subplot.

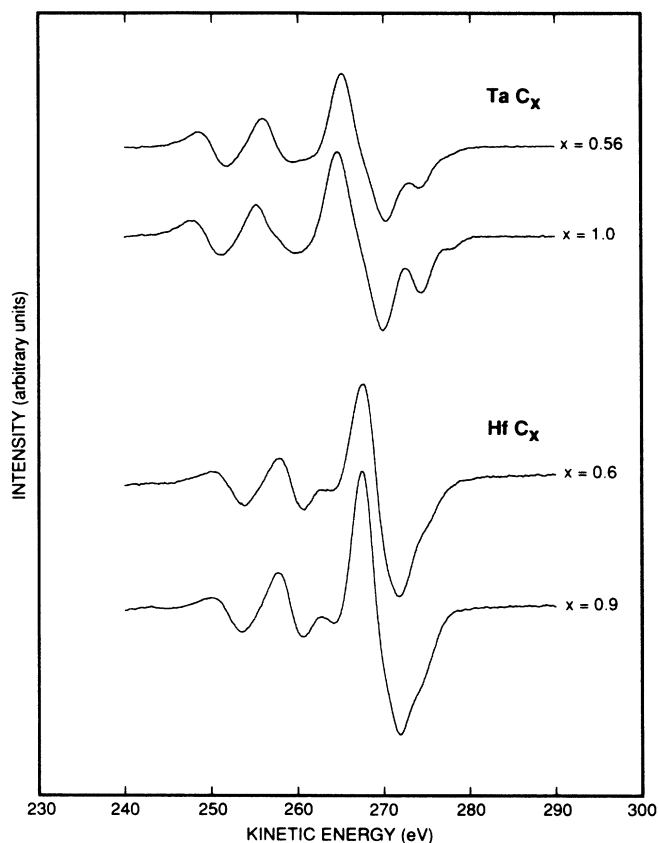


FIG. 6. C *KVV* Auger spectra from surfaces of TaC_x and HfC_x having different carbon-to-metal ratios x . The spectra are normalized so that the peak-to-peak intensities of the low-energy feature near 250 eV are equal.

creases. For example, from the data shown in Fig. 6, one finds that the ratio of the peak-to-peak intensity of the main feature to that of the small feature near 250 eV decreases from ~ 5.2 for $\text{TaC}_{1.0}$ to ~ 4.3 for $\text{TaC}_{0.56}$ and from ~ 7.7 for $\text{HfC}_{0.9}$ to ~ 6.2 for $\text{HfC}_{0.6}$. Moreover, none of the features broaden as x decreases.

The lower- and higher-energy portions of these spectra arise from transitions involving C *2s* and C *2p* electrons, respectively.¹⁰ The occupancy of the *2s* band, the shape of this band, and the probability of its electrons participating in the Auger process are not expected to change appreciably with x . Hence, the decrease in relative intensity of the higher-energy portions of the spectra with decreasing x must be due in part to a reduction in the number of C *2p* electrons participating in the Auger process per carbon atom.

These changes in the Auger spectra that occur with changing x suggest a reduction in the electron occupancy of the C *2p* band per carbon atom remaining in the solid as the carbon content decreases. That is, the electron charge decreases in the vicinity of the carbon ions as x decreases. This conclusion supports our interpretation, presented in Sec. IV C, concerning changes in the charge distribution accompanying changes in the carbon-to-metal ratio x .

IV. DISCUSSION

At first glance, it appears that whatever is happening in hafnium carbide is quite different from whatever is happening in tantalum carbide. Consider four differences suggested by the data.

(i) The C *1s* BE in stoichiometric TaC is ~ 282.9 eV; in stoichiometric HfC, it is ~ 281.55 eV, ~ 1.35 eV smaller [cf. Figs. 2(b) and 3(b)].

(ii) The Ta *4f* BE in elemental Ta is ~ 2.0 eV smaller than it is in stoichiometric TaC; the Hf *4f* BE in elemental Hf is ~ 0.05 eV larger than it is in stoichiometric HfC [cf. Figs. 2(a) and 3(a)].

(iii) As x decreases, the metal and carbon BE's and the BE of the main *p-d* valence-band peak decrease in TaC_x but increase in HfC_x .

(iv) As x decreases, the shape of the valence-band spectra for HfC_x changes very little, whereas for TaC_x the relative intensity just below E_F increases significantly and eventually becomes the dominant intensity of the spectra.

In the remainder of this section the origin of these four differences in the data is discussed. We consider the ~ 1.35 -eV difference between C *1s* BE's in Sec. IV A, the differences between *4f* BE's in the elemental metals and corresponding stoichiometric carbides in Sec. IV B, and the two differences noted in the behavior of TaC_x and HfC_x in Sec. IV C. Concluding remarks are made in Sec. V.

Before proceeding to Sec. IV A, four preliminary comments will be made. First, it will prove useful in thinking through the physics to reference energy levels to the crystal zero. In this regard it is helpful to define the crystal zero as that energy level which differs from the vacuum zero only by a surface-barrier potential arising from the surface dipole. The position of the crystal zero cannot be determined experimentally; it is used here only as a conceptual aid, and its use is justified only insofar as it is helpful. We find it helpful for two reasons: It is a property of the bulk material, and it is not tied to the Fermi level (why this second reason is helpful will become clear beginning in the following paragraph). Operationally, we will use a less exact definition and consider the crystal zero as being tied to the bulk valence band. The subject of choosing a reference zero is discussed further in Sec. IV C 1.

Second, it also will prove useful to consider differences in binding energies as arising from differences both in the core-level energies themselves and in the Fermi levels. In such discussions, energy levels are referenced to the crystal zero. Core-level and Fermi-level differences, of course, often are no more than two aspects of the same phenomenon. Delineating binding-energy differences in terms of them, however, will prove helpful in understanding those factors responsible for the binding-energy differences; this approach also will prove helpful in understanding the origins of differences in the valence-band spectra of TaC_x and HfC_x . Even though differences in Fermi levels, core levels, and valence bands are discussed separately in what follows, the reader should keep their interrelationship in mind.

Third, it will become apparent that core-level shifts are

being interpreted as arising from changes in the amount of negative charge in the vicinity of the core electrons in question. It is recognized that other factors contribute to core-level shifts,¹¹ yet, for these carbides we contend that such charge-distribution changes play the major role.

Finally, energy differences in this paper refer to “TaC minus HfC,” “Ta minus Hf,” or “carbide minus elemental material,” whichever is appropriate.

A. Difference in C 1s BE's in the stoichiometric carbides

As indicated above, the ~ 1.35 -eV difference in C 1s BE's between carbon in TaC and carbon in HfC can be considered as arising from differences both in the C 1s levels and in the Fermi levels themselves. If these differences are given by Δ_{1s} and $\Delta_{E_F}^{\text{carbides}}$, respectively, then the ~ 1.35 -eV difference in BE's can be written as follows:

$$\sim 1.35 \text{ eV} = \Delta_{E_F}^{\text{carbides}} - \Delta_{1s}, \quad (1)$$

where $\Delta_{E_F}^{\text{carbides}}$ and Δ_{1s} are defined as the level in TaC minus the level in HfC. Convention would have us line up the two Fermi levels so that $\Delta_{E_F}^{\text{carbides}} = 0$ and $\Delta_{1s} \simeq -1.35$ eV. We could equally well line up the 1s levels and obtain $\Delta_{1s} = 0$ and $\Delta_{E_F}^{\text{carbides}} \simeq 1.35$ eV. As indicated above, however, we choose to think in terms of lining up the crystal zeros. What we have in mind is presented schematically in Fig. 7.

A rough estimate of $\Delta_{E_F}^{\text{carbides}}$ can be made. We first note that the geometric structures of HfC and TaC are the same (NaCl) and that their band structures are similar.¹² In fact, the energy bands can be considered as being nearly rigid upon going from *stoichiometric* HfC to *stoichiometric* TaC, in that a main difference in their electronic structures is that TaC has an additional electron per unit cell and hence its Fermi level lies higher in its bands. If one assumes that the energy bands of HfC and

TaC are similarly positioned with respect to their crystal zeros, one might estimate the difference in Fermi levels $\Delta_{E_F}^{\text{carbides}}$ as $1/N_{\text{carbides}}(E_F) \simeq 2.2$ eV, where $N_{\text{carbides}}(E_F) = [N_{\text{TaC}}(E_F) + N_{\text{HfC}}(E_F)]/2$ is a simple average of the density of states of these carbides at the Fermi level, $N_M(E_F)$ is the density of states of material M at the Fermi level, and values in Table II have been used. Looking more carefully at the density of states¹² of HfC and TaC may suggest that this estimate ($\Delta_{E_F}^{\text{carbides}} \simeq 2.2$ eV) is a little low, but it cannot be too far off. It follows from Eq. (1) that $\Delta_{1s} \simeq 0.85$ eV, where, again, the estimate is probably low.

The result $\Delta_{1s} > 0$ means that the C 1s level is higher in TaC than in HfC, as depicted in Fig. 7. We interpret this result as suggesting that there is more electron charge in the vicinity of carbon ions in stoichiometric TaC than in stoichiometric HfC. Note that if BE differences were equated to core-level differences, i.e., if the effect of Fermi-energy differences were ignored, one may have reached just the opposite conclusion. Note, too, that a larger charge transfer occurring during the formation of TaC would not be consistent with traditional notions concerning differences in electronegativity. Conventional wisdom would have Hf more electropositive than Ta and, therefore, would have the larger charge transfer onto carbon occurring during the formation of HfC. The result $\Delta_{1s} > 0$, however, may have little to do with charge transfer in the sense of charge initially localized on one site becoming localized on a second site; some of the charge residing in the neighborhood of carbon sites arises from the tails of wave functions centered on metal sites, and recent work¹⁴ suggests that the tailing should be larger in TaC than in HfC.

We now obtain Eq. (1) in a way that parallels the approach used below in our consideration of $4f$ BE's in the elemental metals and corresponding carbides. The difference in C 1s BE's between carbon in graphite¹⁵ (~ 284.3 eV) and carbon in TaC (~ 282.9 eV BE) is about -1.4 eV. As before, this -1.4 -eV difference can be considered as arising from two factors, one due to a difference in Fermi levels plus one due to a difference in carbon levels:

$$-1.4 \text{ eV} \simeq E_F^{\text{TaC}} - E_F^{\text{C}} - \delta E_{1s}^{\text{TaC}}. \quad (2)$$

The chemical shift $\delta E_{1s}^{\text{TaC}}$ includes all energies attributable to the differences in carbon environments (new positions of carbon potentials, presence of tantalum poten-

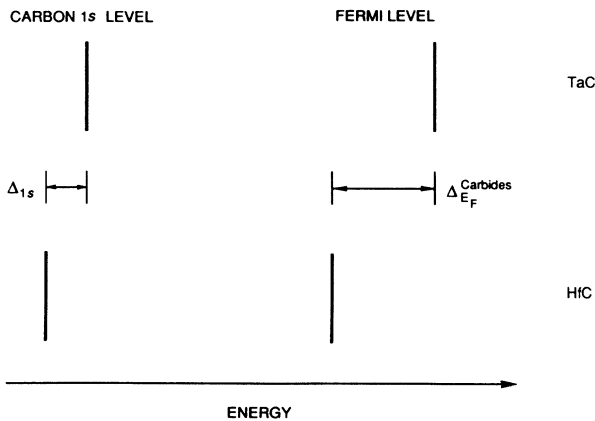


FIG. 7. Schematic energy diagram depicting Δ_{1s} and $\Delta_{E_F}^{\text{carbides}}$ for stoichiometric TaC and HfC. As shown, these energy differences are positive (defined as “TaC minus HfC”). Energy levels are referenced to respective crystal zeros.

TABLE II. Density of states $N_M(E_F)$ in eV^{-1} of material M at the Fermi level E_F .

Material	$N_M(E_F)$
TaC	0.56 ^a
HfC	0.33 ^a
Ta	1.26 ^b
Hf	0.49 ^b

^aReference 12.

^bReference 13.

tials, and so on) and is equal to the C 1s level in TaC minus that in graphite, where energy levels are referenced to the respective crystal zeros. Equation (2) is presented schematically in Fig. 8(a). A similar equation can be written for the -2.75 -eV difference in C 1s BE's between carbon in graphite (~ 284.3 eV BE) and carbon in HfC (~ 281.55 eV BE):

$$-2.75 \text{ eV} \approx E_F^{\text{HfC}} - E_F^{\text{C}} - \delta E_{1s}^{\text{HfC}}. \quad (3)$$

Equation (3) is presented schematically in Fig. 8(b). One obtains Eq. (1) by subtracting Eq. (3) from Eq. (2) and setting Δ_{1s} equal to the difference in chemical shifts: $\Delta_{1s} = \delta E_{1s}^{\text{TaC}} - \delta E_{1s}^{\text{HfC}}$.

B. Differences between 4f BE's in the elemental metals and corresponding stoichiometric carbides

The ~ 2 -eV difference in Ta 4f BE's between Ta in elemental Ta and Ta in TaC can be considered similarly as arising from a difference in Fermi levels plus a difference in tantalum levels. What we have in mind is shown in the top of Fig. 9. In symbols we write

$$2 \text{ eV} \approx E_F^{\text{TaC}} - E_F^{\text{Ta}} - \delta E_{\text{Ta } 4f}^{\text{TaC}}, \quad (4)$$

where the chemical shift $\delta E_{\text{Ta } 4f}^{\text{TaC}}$ includes all energies arising from the differences in the Ta environments and is equal to the Ta 4f level in TaC minus that in elemental Ta. As before, all energies are referenced to the appropriate crystal zero. A similar equation can be written for the ~ 0.05 -eV difference in Hf 4f BE's between Hf in elemental Hf and Hf in HfC:

$$-0.05 \text{ eV} \approx E_F^{\text{HfC}} - E_F^{\text{Hf}} - \delta E_{\text{Hf } 4f}^{\text{HfC}}. \quad (5)$$

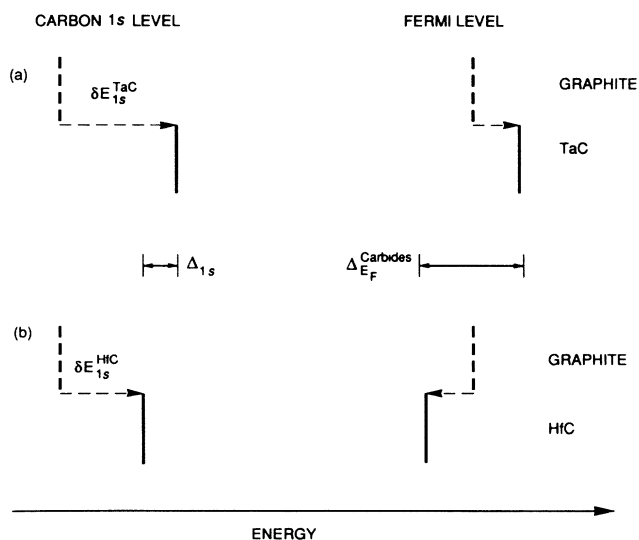


FIG. 8. Schematic energy diagram depicting Δ_{1s} , $\Delta_{EF}^{\text{carbides}}$, and the chemical shifts $\delta E_{1s}^{\text{TaC}}$ and $\delta E_{1s}^{\text{HfC}}$. As shown, these energy differences are positive (defined as "TaC minus HfC" or "carbide minus elemental material"). Unlabeled energy differences are not relevant to the present discussion. Energy levels are referenced to respective crystal zeros.

This equation is presented schematically in the bottom of Fig. 9. Subtracting Eq. (5) from Eq. (4) yields

$$2.05 \text{ eV} \approx \Delta_{EF}^{\text{carbides}} - \Delta_{EF}^{\text{metals}} + \Delta_{1s}, \quad (6)$$

where $\Delta_{EF}^{\text{metals}} = E_F^{\text{Ta}} - E_F^{\text{Hf}}$, and where we have approximated the difference of chemical shifts for the metal atoms $\delta E_{\text{Ta } 4f}^{\text{TaC}} - \delta E_{\text{Hf } 4f}^{\text{HfC}} \equiv \Delta_{4f}$ as being equal to the negative of the difference of chemical shifts for the carbon atoms. Note that Δ_{1s} appears with a positive sign in Eq. (6) and with a negative sign in Eq. (1) because the changes in the electron charge distributions accompanying the formation of these materials tend to shift carbon and metal levels in opposite directions. By adding Eqs. (1) and (6), and using the estimate $\Delta_{EF}^{\text{carbides}} \approx 2.2$ eV, one obtains $\Delta_{EF}^{\text{metals}} \approx 1$ eV.

It would be instructive to determine whether or not $\Delta_{EF}^{\text{metals}} \approx 1$ eV makes sense. It would be difficult, however, to justify estimating $\Delta_{EF}^{\text{metals}}$ by the method used in Sec. IV B to estimate $\Delta_{EF}^{\text{carbides}}$, because both the crystal structure and the electronic structure of Hf differ markedly from those of Ta. That method would give a Fermi-energy increase upon going from Hf to Ta of about $1/N_{\text{metals}}(E_F) \approx 1.1$ eV, where $N_{\text{metals}}(E_F) = [N_{\text{Ta}}(E_F) + N_{\text{Hf}}(E_F)]/2$ and where values in Table II have been

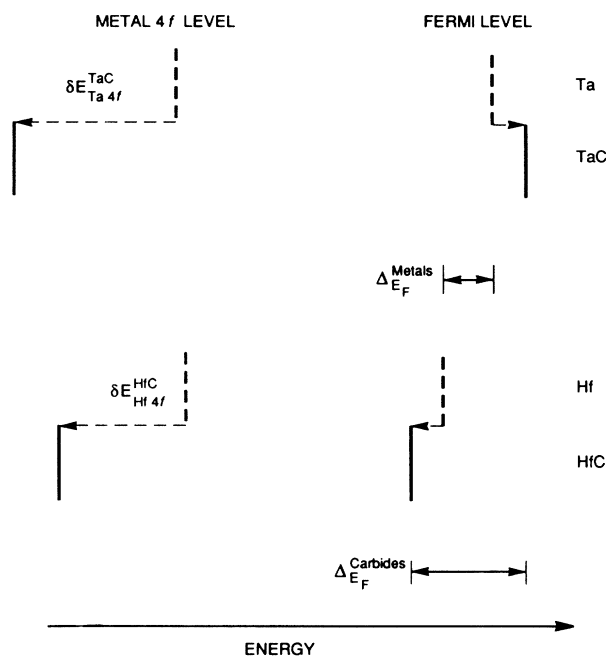


FIG. 9. Schematic energy diagram depicting the effect of Fermi-level and core-level shifts upon the Ta 4f and Hf 4f BE's. As shown, $\Delta_{EF}^{\text{metals}}$ and $\Delta_{EF}^{\text{carbides}}$ are positive (defined as "Ta minus Hf" and "TaC minus HfC," respectively), but the chemical shifts $\delta E_{\text{Ta } 4f}^{\text{TaC}}$ and $\delta E_{\text{Hf } 4f}^{\text{HfC}}$ are negative (defined as "carbide minus elemental material"). Unlabeled energy differences are not relevant to the present discussion. Energy levels are referenced to respective crystal zeros. The connection between this figure and Fig. 8 should be noted.

used. The point of this section, however, is not to obtain quantities such as $\Delta_{E_F}^{\text{metals}}$ —the good agreement between $1/N_{\text{metals}}(E_F)$ and $\Delta_{E_F}^{\text{metals}}$ is quite fortuitous, owing to the crudeness and uncertainties of the approximations involved—but rather to show that the differences in the metal 4*f* BE's can be interpreted without invoking substantial differences between the charge transfer accompanying the formation of HfC and that accompanying the formation of TaC (which one would be tempted to do if the C 1*s* spectra were not available).

C. Differences between TaC_x and HfC_x accompanying changes in *x*

1. The choice of a reference potential

We propose that the XPS data summarized in Fig. 5 can be understood in terms of changes in the charge distributions accompanying changes in *x*. In particular, we propose that, as *x* decreases for either TaC_x and HfC_x, the electron charge increases in the vicinity of the metal ions and decreases in the vicinity of the carbon ions. This view is elucidated by choosing a reference potential for which, as *x* decreases, the metal levels go up and the carbon level goes down. A reference potential tied to the *p-d* valence-band peak accomplishes this task satisfactorily. Using this reference potential, one finds that, as the carbon-to-metal ratio decreases from *x* ≈ 1 to *x* ≈ 0.6, the Fermi level decreases by ~0.45 eV in TaC_x and increases by ~0.35 eV in HfC; the metal 4*f* level increases by ~0.2 eV in TaC_x and by ~0.15 eV in HfC_x; and the C 1*s* level decreases by ~0.2 eV in TaC_x and by ~0.05 eV in HfC_x. These results are presented schematically in Fig. 10. As indicated, all energies are referenced with respect to the *p-d* valence-band peak. We note, however, that a reasonable and consistent view of our data ensues if one supposes that this peak shifts very little with respect to the crystal zero as the carbon content is varied. In fact, it is from this perspective that one most clearly sees that

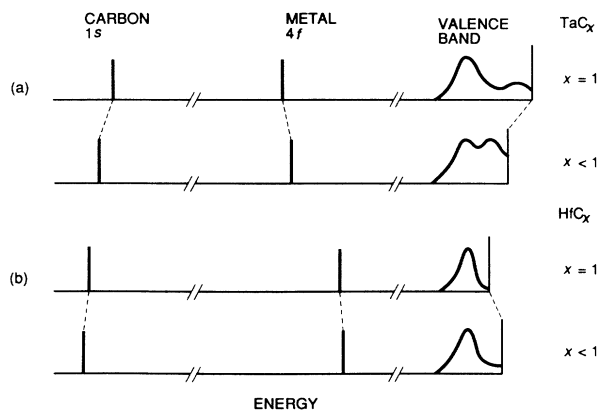


FIG. 10. Schematic of XPS results presented in this paper with the energies referenced to the *p-d* valence-band peak. The vertical (ordinate) axis at the far right of each subplot denotes the position of E_F .

the changes occurring within HfC_x and TaC_x are quite similar. Particularly relevant in this regard are recent work-function measurements¹⁶ that strongly support the supposition concerning the *p-d* valence-band peak being tied to the crystal zero.

2. A closer look at the charge redistribution

Using the energy-level variations given in the above paragraph and the estimates $\Delta_{E_F}^{\text{carbides}}(x \approx 1) \approx 2.2$ eV, $\Delta_{1s}(x \approx 1) \approx 0.85$ eV, and $\Delta_{4f}(x \approx 1) \approx -0.85$ eV made in Secs. IV A and IV B, values of $\Delta_{E_F}^{\text{carbides}}$, Δ_{1s} , and Δ_{4f} for *x* ≈ 0.6 can be obtained. These are given in Table III along with the *x* ≈ 1 estimates. The result $\Delta_{1s}(x) > 0$ suggests that more electron charge is in the vicinity of carbon ions in TaC_x than in HfC_x over the range of *x* considered. Similarly, the result $\Delta_{4f}(x) < 0$ would suggest that the depletion of electron charge in the vicinity of metal ions upon going from elemental Ta to TaC_x is greater than that upon going from elemental Hf to HfC_x over the range of *x* considered; the reader is reminded, however, that the result $\Delta_{4f}(x) < 0$, though plausible, relies upon the approximation $\Delta_{4f}(x = 1) = -\Delta_{1s}(x = 1)$ made in Sec. IV B. Note that the two results $\Delta_{1s}(x) > 0$ and $\Delta_{4f}(x) < 0$ taken together would suggest that, over the range of *x* considered, the charge transfer occurring upon the formation of TaC_x is larger than that of HfC_x.

Our interpretation of the XPS core-level data summarized in Fig. 10 is that, as *x* decreases, the ionicity of both HfC_x and TaC_x is reduced because the electron charge increases in the vicinity of the metal ions and decreases in the vicinity of the carbon ions. This latter point is consistent with our interpretation of the Auger data: There is a depletion of C 2*p* electrons per carbon atom as *x* decreases. The increase in energy of the metal core levels and the decrease in energy of the carbon core levels arise, respectively, from the increase of negative charge in the vicinity of the metal core electrons and the decrease of negative charge in the vicinity of carbon core electrons. Because the separation between carbon and metal levels increases with decreasing *x* more in TaC_x than in HfC_x, in some sense the total redistribution of charge occurring with changing *x* must be larger in TaC_x than in HfC_x.

The charge accumulating in the vicinity of metal ions with decreasing *x* does not arise solely from the charge that is depleted from the vicinity of the carbon ions, which we designate “depleted charge.” To see why this is so, recall that when hafnium carbide or tantalum carbide is formed, charge transfers from metal atoms to carbon

TABLE III. Estimates of $\Delta_{E_F}^{\text{carbides}}$, Δ_{1s} , and Δ_{4f} for metal-to-carbon ratios *x* ≈ 1.0 and *x* ≈ 0.6.

	<i>x</i> ≈ 1.0	<i>x</i> ≈ 0.6
$\Delta_{E_F}^{\text{carbides}}$	2.2	1.4
Δ_{1s}	0.85	0.7
Δ_{4f}	-0.85	-0.8

atoms. Thus, when a carbon vacancy is created, charge that would have transferred to the removed carbon atom from its metal neighbors remains in the crystal. We designate this charge "excess charge," and propose that, along with the depleted charge, it contributes to the total charge accumulating in the vicinity of metal ions as x decreases.

So, two sources for the accumulation of charge in the vicinity of the metal ions have been identified: (1) the depleted charge and (2) the excess charge. Because the Auger spectra of HfC_x and TaC_x change similarly with changing x , it is likely that the contribution from the first source is similar in both sets of materials. Consequently, if the total redistribution of charge occurring with changing x is larger in TaC_x than in HfC_x , as proposed two paragraphs above, then the second source (that of excess charge) must be larger in TaC_x . This conclusion is consistent with $\Delta_{1s}(x) > 0$, in that the inequality suggests more electron charge is in the vicinity of carbon ions in TaC_x than in HfC_x , and hence more excess charge is available to transfer back to the Ta ions when a carbon vacancy is created.

3. Valence-band changes

In HfC_x the charge accumulations discussed above cause relatively little redistribution of Hf states below $E_F(x)$; that is, at least as far as can be discerned from XPS, the bands near E_F appear to behave approximately as rigid bands, and $E_F(x)$ increases as x decreases [as shown in Fig. 10(b)]. In TaC_x , however, there is a significant redistribution of Ta states, with more states being created than destroyed below the original Fermi level; hence, $E_F(x)$ decreases in TaC_x as x decreases [as shown in Fig. 10(a)]. The "extra" intensity lying just below $E_F(x)$ in the valence-band spectra of TaC_x is due to photoemission from metal states that have been significantly redistributed owing to the accumulation of additional charge.

It has been noted that the band structure of HfC is similar to that of TaC and that it can even be considered as being nearly rigid upon going from one stoichiometric material to another. One may wonder, therefore, why changes in the carbon concentration can have such different effects upon the shape of the valence-band spectra in these two materials. We suggest that Fermi-energy differences account for this apparent discrepancy. In particular, we suggest that the new states resulting from the charge redistribution have approximately the same energy in both materials with respect to the p - d valence-band peak, but that they lie above E_F in HfC_x and below E_F in TaC_x . It would be interesting to perform inverse-photoemission or electron-energy-loss measurements on HfC_x to probe the unfilled valence band for such states.

A contributing factor may involve the Hf d 's exhibiting less tailing than the Ta d 's,¹⁴ which may lead to less charge overlap and hence less interaction "across" the carbon vacancy in HfC_x .

V. CONCLUDING REMARKS

Valence-band structures, core-level BE's, and C KVV Auger spectra were obtained for HfC_x ($0.6 \lesssim x \lesssim 1.0$) and TaC_x ($0.5 \lesssim x \lesssim 1.0$), and core-level BE's were obtained for the elemental metals Hf and Ta. A consistent and reasonable explanation of these data results from the following suppositions.

(i) Upon formation of the carbides, the electron charge increases in the vicinity of carbon ions and decreases in the vicinity of metal ions. Over the range of x considered, more charge resides in the vicinity of carbon ions in TaC_x than in HfC_x ; it is likely that TaC_x is more ionic than HfC_x .

(ii) For both TaC_x and HfC_x , as x decreases, the electron charge increases in the vicinity of metal ions and decreases in the vicinity of carbon ions.

(iii) The increase in electron charge in the vicinity of metal ions that accompanies a decrease in x is larger in TaC_x than in HfC_x , whereas the corresponding depletion of charge from carbon ions is approximately equal in the two sets of materials.

(iv) In HfC_x the charge redistribution accompanying changes in x causes relatively little redistribution of Hf states below $E_F(x)$ —the valence band near E_F behaves like a rigid band—and $E_F(x)$ moves higher in the bands with decreasing x . Presumably, there is a significant redistribution of Hf states just above $E_F(x)$.

(v) In TaC_x this charge redistribution causes a significant redistribution of Ta states below $E_F(x)$, with more states being created than destroyed below the original Fermi level, and $E_F(x)$ moves lower in the bands with decreasing x .

It is the difference in valence-band behavior described in (iv) and (v), and not some significant difference in charge distributions, that is primarily responsible for the spectroscopic data of HfC_x differing from those of TaC_x .

ACKNOWLEDGMENTS

We thank J. B. Bates, R. A. DiDio, and G. D. Mahan for their useful comments and a careful reading of the paper, and G. W. Ownby for his technical assistance. This research was sponsored by the Division of Materials Sciences, U.S. Department of Energy, under Contract No. DE-AC05-84OR21400 with Martin Marietta Energy Systems, Inc.

¹Books and review articles on the carbides include the following: E. K. Storms, *The Refractory Carbides*, edited by J. L. Margrave (Academic, New York, 1967); L. E. Toth, *Transition Metal Carbides and Nitrides*, edited by J. L. Margrave

(Academic, New York, 1971); W. S. Williams, in *Progress in Solid State Chemistry*, edited by H. Reiss and J. O. McCaldin (Pergamon, New York, 1972), Vol. 6, p. 57; S. T. Oyama and G. L. Haller, in *Catalysis*, Vol. 5 of *Specialist Periodical Re-*

- ports, edited by G. C. Bond and G. Webb (Royal Society of Chemistry, London, 1982), p. 333.
- ²For a review of both theoretical and experimental work in the area of electronic structure, see A. Neckel, *Int. J. Quantum Chem.* **23**, 1317 (1983).
- ³G. R. Gruzalski and D. M. Zehner, *Phys. Rev. B* **34**, 3841 (1986).
- ⁴C. J. Powell, B. E. Erikson, and T. Jach, *J. Vac. Sci. Technol.* **20**, 625 (1982).
- ⁵C. D. Wagner, W. M. Riggs, L. E. Davis, J. F. Moulder, and G. E. Muilenberg, in *Handbook of X-Ray Photoelectron Spectroscopy*, edited by B. E. Muilenberg (Perkin-Elmer Corp., Eden Prairie, MN, 1979), p. 188.
- ⁶C. Oshima, R. Soudia, M. Aono, S. Otani, and Y. Ishizawa, *Phys. Rev. B* **30**, 5461 (1984).
- ⁷H. G. Smith and W. Glaser, *Phys. Rev. Lett.* **25**, 1611 (1970).
- ⁸Compare, for example, with valence-band spectra obtained from polycrystalline HfC and TaC using monochromatic x rays and presented by H. Ihara, M. Hirabayashi, and H. Nakagawa, *Phys. Rev. B* **14**, 1707 (1976).
- ⁹G. H. Schadler, A. M. Boring, P. Weinberger, and A. Gonis, *Phys. Rev. B* **38**, 9538 (1988).
- ¹⁰G. R. Gruzalski, D. M. Zehner, and G. W. Ownby, *Surf. Sci.* **157**, L395 (1985).
- ¹¹See, for example, R. E. Watson and M. L. Perlman, in *Structure and Bonding*, edited by J. D. Dunitz, P. Hemmerich, R. H. Holm, J. A. Ibers, C. K. Jorgensen, J. B. Neilands, D. Reinen, and R. J. P. Williams (Springer-Verlag, New York, 1975), Vol. 24, pp. 83–132; *Phys. Scr.* **21**, 527 (1980).
- ¹²B. M. Klein, D. A. Papaconstantopoulos, and L. L. Boyer, *Phys. Rev. B* **22**, 1946 (1980).
- ¹³D. A. Papaconstantopoulos, *The Band Structure of Elemental Solids* (Plenum, New York, 1986).
- ¹⁴R. E. Watson, J. W. Davenport, and M. Weinert, *Phys. Rev. B* **35**, 508 (1987); **36**, 6396 (1987).
- ¹⁵K. Hamrin, G. Johannsson, U. Gelius, C. Nordling, and K. Siegbahn, *Phys. Scr.* **1**, 277 (1970). Note that the actual value of the C 1s BE in graphite is not needed in this discussion.
- ¹⁶G. R. Gruzalski, S.-C. Lui, and D. M. Zehner (unpublished).